



HAL
open science

Ultimate tensile strength during fatigue of fiber-reinforced ceramic-matrix composites

François Hild, Alain Burr

► **To cite this version:**

François Hild, Alain Burr. Ultimate tensile strength during fatigue of fiber-reinforced ceramic-matrix composites. *Mechanics Research Communications*, 1995, 22 (4), pp.401-406. 10.1016/0093-6413(95)00042-P . hal-01636225

HAL Id: hal-01636225

<https://hal.science/hal-01636225>

Submitted on 31 Oct 2019

HAL is a multi-disciplinary open access archive for the deposit and dissemination of scientific research documents, whether they are published or not. The documents may come from teaching and research institutions in France or abroad, or from public or private research centers.

L'archive ouverte pluridisciplinaire **HAL**, est destinée au dépôt et à la diffusion de documents scientifiques de niveau recherche, publiés ou non, émanant des établissements d'enseignement et de recherche français ou étrangers, des laboratoires publics ou privés.

ULTIMATE TENSILE STRENGTH DURING FATIGUE OF FIBER-REINFORCED CERAMIC-MATRIX COMPOSITES

Alain Burr and François Hild

Laboratoire de Mécanique et Technologie,
E.N.S. de Cachan / C.N.R.S. / Université Paris 6
61 avenue du Président Wilson, F-94235 Cachan Cedex, France.

Introduction

The aim of this paper is to derive the ultimate tensile strength during fatigue loading of fiber-reinforced ceramic-matrix composites. Two different phenomena arise as a consequence of fatigue loading. First, wear may take place at the fiber/matrix interface [1]. Second, fiber embrittlement can occur at intermediate temperatures [2] as a result of oxidation. At room temperature, however, only the first phenomenon takes place. Estimate of the effect of cyclic loading on the ultimate tensile strength is possible when the influence of interfacial wear is included in the model. It is shown that the ultimate strength is defined by means of a shear strength map with three different regimes.

Ultimate Tensile Strength

The ultimate tensile strength properties of fiber-reinforced ceramic-matrix composites (CMC's) are usually dictated by the strength of the fibers. The fibers exhibit a statistical variation of strength that obeys a two-parameter Weibull law. Provided the fibers are subject to global load

sharing, the load transmitted from each failed fiber is shared equally among the intact fibers, the ultimate tensile strength is then scaled by a characteristic strength [3] S_c according to

$$\bar{\sigma}_{UTS} = f S_c F(m), \quad \text{with } S_c^{m+1} = \frac{L_0 S_0^m \tau}{R_f} \quad (1)$$

where f is the fiber volume fraction, m the shape parameter, S_0 the stress scale parameter, L_0 a gauge length, τ the interfacial shear resistance, and R_f the fiber radius. The function F depends upon the shape parameter m and whether localization happens or not before the peak stress [4-6]. To assess the ultimate tensile strength, the function F is given by [4]

$$F(m) = \left(\frac{2}{m+2} \right)^{1/(m+1)} \frac{m+1}{m+2} \quad (2.1)$$

and to calculate the localization tensile strength, the function F can be written as [6]

$$F(m) = \frac{1}{2} \left(\frac{1}{m+1} \right)^{1/(m+1)} \left\{ 1 + \exp\left(-\frac{1}{m+1}\right) \right\} \quad (2.2)$$

Eqn. (1) shows that the interfacial shear resistance τ is a key parameter. If wear is involved, it is expected that τ decreases as the number of cycles increases.

Shear Stress Evolution

When push-pull experiments are performed on CMC's, it is known that the first cycle is often the most damaging in reducing of shear stress [1]. Therefore, following the first reversal of sliding, the frictional shear stress is assumed to decrease from τ_0 to τ_∞ . The density of matrix cracks is defined by a crack spacing $2L$. Upon first loading to a maximum stress σ , a friction length $2L_{F0}$ is reached ($L_{F0} \leq L$) over which the shear strength is equal to τ_0 (Fig. 1).

Upon unloading to $\sigma - \Delta\sigma = R\sigma$ a shear stress reversal occurs over a length L_{U1} , for which the interfacial shear strength is equal to τ_∞ . Upon reloading to σ there is shear stress reversal over the length L_{U1} for which the interfacial shear strength is still τ_∞ ; together with σ , sliding evolves from L_{F0} to L_{F1} , for which the interfacial shear stress is τ_0 . As the number of cycles N increases, there is an increase of $L_{F(N+1)}$ and $L_{U(N+1)}$ given by ($N \geq 1$)

$$-\frac{2\tau_\infty}{R_f} L_{U(N+1)} + \frac{2\tau_0}{R_f} (L_{FN} - L_{U(N+1)}) = \frac{(1-f)E_m}{fE} R\sigma \quad (3.1)$$

$$\frac{2\tau_{\infty}}{R_f} L_{U(N+1)} + \frac{2\tau_0}{R_f} (L_{F(N+1)} - L_{U(N+1)}) = \frac{(1-f)E_m}{fE} \sigma \quad (3.2)$$

with $L_{F0} = \frac{(1-f)E_m \sigma R_f}{2fE\tau_0}$, where E_m (resp. E) is the Young's modulus of the matrix (resp. composite). So that the following expressions can be expressed as a function of accumulated number of cycles ($N \geq 0$)

$$L_{FN} = \frac{(1-f)E_m \sigma R_f}{2fE\tau_0} + \gamma(1-R) \frac{(1-f)E_m \sigma R_f}{2fE\tau_0} \frac{1-\gamma^N}{1-\gamma}, \quad L_{UN} = \frac{(1-R)(1-f)E_m \sigma R_f}{4fE\tau_0} (1+\gamma) \frac{1-\gamma^N}{1-\gamma} \quad (4)$$

with $\gamma = \frac{\tau_0 - \tau_{\infty}}{\tau_0 + \tau_{\infty}}$, $0 < \gamma < 1$. The case $\gamma = 0$ does not deal with fatigue wear. The case $\gamma = 1$ is trivial to study and can be described by an arithmetic sequence instead of a geometric one for L_{FN} and L_{UN} .

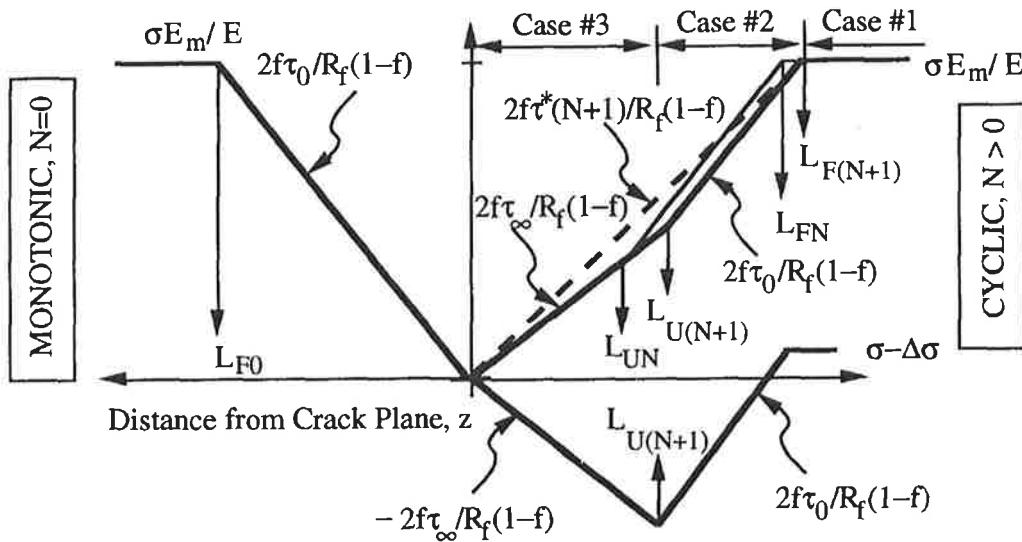


Fig. 1 : Stress profile in the matrix. Depiction of the three different cases.

The symbol  denotes the slope of a pointed straight line.

The stress profile in the matrix is plotted in Fig. 1. Provided subcritical crack propagation does not exist, there is no further matrix cracking under cyclic loading conditions. However, fiber

breakage may occur since the longitudinal stress in the fibers increases as a result of wear. In the following, we will neglect this phenomenon.

There are three cases to be considered. In case #1, $L > L_{FN}$, the condition for matrix cracking saturation is not reached. For case #2, $L_{UN} \leq L \leq L_{FN}$, matrix cracking saturation occurs and the friction characteristics involve τ_0 and τ_∞ . For case #3, $L_{UN} > L$, matrix cracking saturation takes place but the friction characteristics only involve τ_∞ . To characterize the features of the shear stress profile, when $N > 0$, an equivalent shear stress $\tau^*(N)$ is defined by

$$\tau^*(N) = \begin{cases} \frac{(1-f)R_f \sigma_m(L_{FN})}{2fL_{FN}} & L > L_{FN} \\ \frac{(1-f)R_f \sigma_m(L)}{2fL} & L \leq L_{FN} \end{cases} \quad (5)$$

where $\sigma_m(z)$ is the tensile stress in the matrix (Fig. 1). This equivalent shear stress is the key parameter used to determine the fatigue properties. The evolution of the latter is given by

$$\frac{\tau^*(N)}{\tau_0} = \begin{cases} \frac{1-\gamma}{1-\gamma R - (1-R)\gamma^{N+1}} & L \geq L_{FN} \\ 1 - \frac{\gamma}{1-\gamma} \frac{(1-R)(1-f)E_m \sigma R_f}{2fE\tau_0 L} (1-\gamma^N) & L_{UN} \leq L < L_{FN} \\ \frac{1-\gamma}{1+\gamma} = \frac{\tau_\infty}{\tau_0} & L < L_{UN} \end{cases} \quad (6)$$

from which the shear stress map shown in Fig. 2 can be obtained. When $N = 0$, $\tau^*(0) = \tau_0$ since no reversal occurred. On the other hand, when $N = +\infty$, since $\gamma < 1$, the maximum value of $\tau^*(\infty) = \tau_0(1-\gamma)/(1-\gamma R)$ and the minimum value of $\tau^*(\infty) = \tau_\infty$. This last result shows that τ_∞ can only be reached if saturation takes place during cycling ($L < L_{F\infty}$) and complete reversal occurs at least one cycle over a length L ($L < L_{U\infty}$).

To determine the ultimate tensile strength when saturation is not reached at the end of N cycles, it is necessary to know the value of the shear stress $\tau^{*-c}(N)$ at cracking saturation. It is greater than the value $\tau^*(N)$ obtained when $L > L_{FN}$, since the friction length increases further under subsequent monotonic loading with a shear stress equal to τ_0 over a range $L_{UN} < z < L_{sat}(N)$, where $L_{sat}(N)$ denotes the average crack spacing at saturation (Fig. 3). It is worth noting that $L_{sat}(N)$ is different from the average crack spacing at saturation under monotonic load conditions obtained by computing $L_{F0} = L$. The quantity $L_{sat}(N)$ also depends upon the number of cycles since cracking occurs only in areas in the matrix where the stresses become higher than the maximum cyclic stress $E_m \sigma/E$, and these areas become smaller as the number of

cycles increases. Therefore, by definition, the value of the shear stress $\tau^{*-c}(N)$ depends upon the number of cycles.

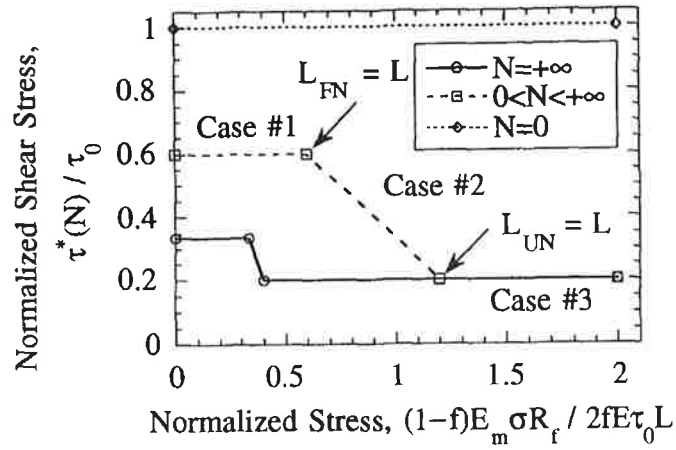


Fig. 2 : Shear stress map after cycling when $\tau_\infty / \tau_0 = 0.2$, $R = 0$.

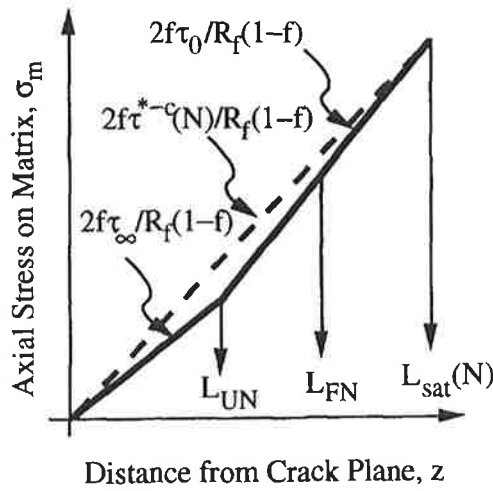


Fig. 3 : Depiction of the three different cases to determine the ultimate strength.

The symbol \curvearrowright denotes the slope of a pointed straight line.

As a consequence, the boundary between case #1 and case #2 is altered owing to the fact that $\tau(N) \geq \tau^*(N)$. A shear stress map to determine the fatigue ultimate tensile strength is plotted in Fig. 4 using the following results when $N > 0$

$$\frac{\tau(N)}{\tau_0} = \begin{cases} 1 - \frac{\gamma}{1-\gamma} \frac{(1-R)(1-f)E_m \sigma R_f}{2fE\tau_0 L_{sat}(N)} (1-\gamma^N) = \frac{\tau^{*-c}(N)}{\tau_0} & L = L_{sat}(N) \\ 1 - \frac{\gamma}{1-\gamma} \frac{(1-R)(1-f)E_m \sigma R_f}{2fE\tau_0 L} (1-\gamma^N) & L_{UN} \leq L < L_{sat}(N) \\ \frac{\tau^*(N)}{\tau_0} = \frac{\tau_\infty}{\tau_0} & L < L_{UN} \end{cases} \quad (7)$$

This map is useful for deriving the ultimate fatigue strength according to Eqn. (1). Under monotonic loading conditions, the value of τ in Eqn. (1) is taken equal to τ_0 , whereas under cyclic loading conditions, it is taken equal to $\tau(N)$. It is worth noting that these results include directly the amplitude effect by the presence of the load ratio R .

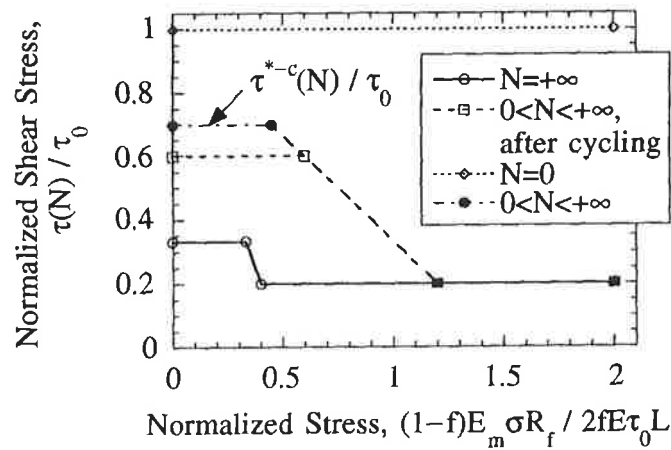


Fig. 4 : Shear stress map when $\tau_\infty / \tau_0 = 0.2$, $R = 0$.

References

1. D. Rouby and P. Reynaud, *Comp. Sci. Tech.*, **48**, 109-118 (1993).
2. E. Bischoff et al., *J. Am. Ceram. Soc.*, **72** (5), 741-745 (1989).
3. R.B. Henstenburg and S.L. Phoenix, *Polym. Comp.*, **10** (5), 389-406 (1989).
4. W.A. Curtin, *J. Am. Ceram. Soc.*, **74** (11), 2837-2845 (1991).
5. W.A. Curtin, *J. Mech. Phys. Solids*, **41** (1), 35-53 (1993).
6. F. Hild and A. Burr, *Mech. Res. Comm.*, **21** (4), 297-302 (1994).